

## Electronic Supplementary Information

### **A high-performance broadband double-junction photodetector based on silicon nanowire arrays wrapped by silver nanoparticles for low-light imaging**

Yuting Huang,<sup>a</sup> Haifeng Liang,<sup>\*b</sup> Yingli Zhang,<sup>a</sup> Shujing Yin,<sup>a</sup> Xuyang Li,<sup>a</sup> Changlong Cai,<sup>a</sup> Weiguo Liu<sup>a</sup> and Tiantian Jia<sup>c</sup>

<sup>a</sup> Key laboratory for optical measurement and thin films of Shaanxi Province, Xi'an Technological University, Xi'an, Shaanxi 710021, China

<sup>b</sup> College of integrated circuits and optoelectronic chips, Shenzhen Technology University, Shenzhen, Guangdong 518118, China

<sup>c</sup> Key Laboratory of Low-Light-Level Night Vision Technology, Xi'an, Shaanxi 710065, China

\*Corresponding author: E-mail: lianghaifeng@xatu.edu.cn

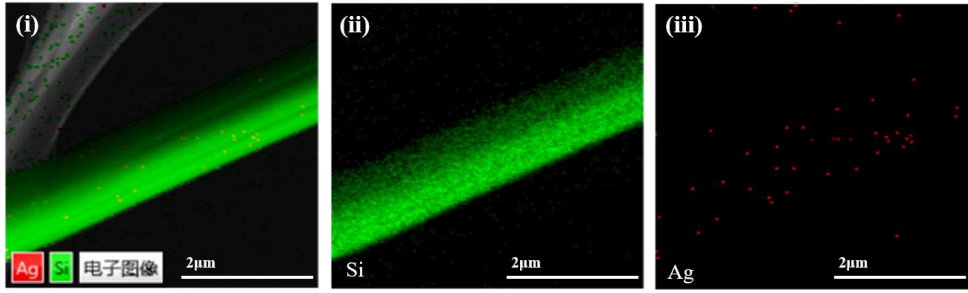


**Fig. S1** Energy spectrum mapping of (i) silicon and silver elements of layer image, (ii) silicon and (iii) silver elements.

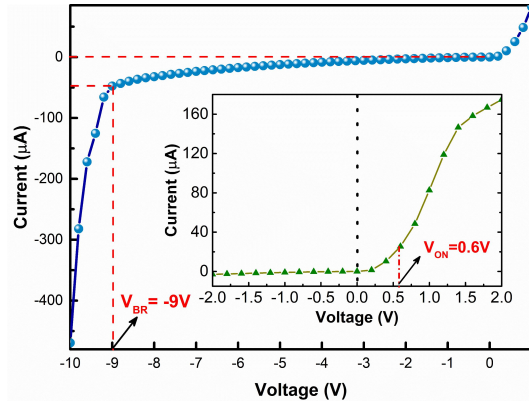


**Fig. S2**  $I$ - $V$  characteristic curve of the device measured in 650 nm irradiation, the breakdown voltage was approximately -9 V, and the inset shows the turn-on voltage was 0.6 V.

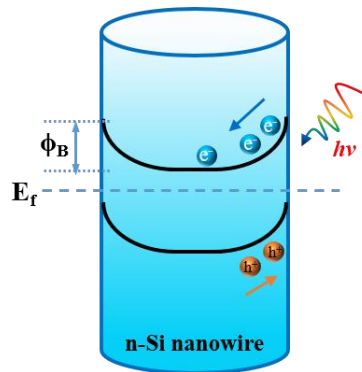


**Fig. S3** Nanowire surface band bending and photogenerated carriers are separated under illumination,  $\phi_B$  the recombination barrier.

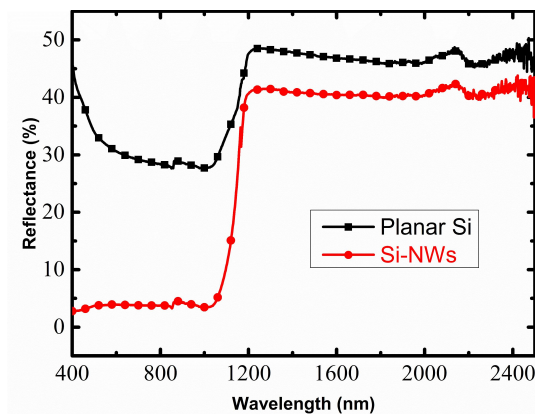


**Fig. S4** UV-vis-NIR reflectance spectra of the SiNW arrays and planar Si.

**Table S1.** Comparison of the typical figure of merits between our NN<sup>+</sup>/MS double junction enhanced SiNWs@AgNPs photodetector and other reported the nanowire silicon-based devices, mainly including  $R$ , Response wavelength range,  $D^*$ ,  $I_{dark}$ , response speed (rise/fall time), and weak light sensitivity (low light intensity that can be detected).

Category	Devices	$R$ [A/W]	Photo- response range [ $\mu\text{m}$ ]	$D^*$ [cm Hz <sup>1/2</sup> /W]	$I_{dark}$ [A]	Rise/fall time [ $\mu\text{s}$ ]	Low power intensity	Ref.
Junction structure	p-SiNWs/nCdS nanoparticles	0.821 @900 nm	0.2-1.1	$1.21 \times 10^{12}$	$\sim 2 \times 10^{-7}$	203 ms/ 429 ms	$8 \mu\text{W}/\text{cm}^2 \sim$ $1 \text{ mW}/\text{cm}^2$	1
	PdSe <sub>2</sub> /SiNWA	0.726 @980 nm	0.2–2	$3.19 \times 10^{14}$	$\sim 10^{-10}$	3.4/3.9	$27.5 \sim 56.6$ $\text{nW}/\text{cm}^2$	2
	MoS <sub>2</sub> /Al <sub>2</sub> O <sub>3</sub> /SiN Ws	0.61 @808 nm	0.3-1.6	$1.48 \times 10^{12}$	$\sim 10^{-9}$	8.4/40.9	$1.4 \text{ nW}/\text{cm}^2 \sim$ $714.3 \text{ mW}/\text{cm}^2$	3
	perovskite nanowires/Au	37.14 @473 nm	0.35-0.9	$2.06 \times 10^{13}$	$\sim 10^{-10}$	91/563	$1.45 \text{ nW}/\text{cm}^2 \sim$ $145 \text{ mW}/\text{cm}^2$	4
plasmonic enhanced detector	AgNP/SiOx NW/Si	1.54 @370nm	0.3-0.85	$2.12 \times 10^{10}$	$\sim 10^{-10}$	0.12s/ 0.11s	/	5
	rGO: AuCQD/Si NW	0.5 @940nm	0.36-0.94	$1.4 \times 10^{12}$	$\sim 10^{-10}$	750ms/ 667ms	$0.2 \mu\text{W}/\text{cm}^2 \sim$ $0.6 \text{ mW}/\text{cm}^2$	6
	MoS <sub>2</sub> /AgNPs/Si NWs	402.4 @532nm	0.405- 0.635	$2.34 \times 10^{12}$	$\sim 10^{-4}$	41ms/ 37ms	$0.13 \sim 231.7$ $\text{mW}/\text{cm}^2$	7
	Au antennas/All- Si	0.05 @980nm	0.8-1.6	$2 \times 10^{11}$	/	/	/	8
	Perovskite/Au squares/Si/SiO	4.2 @800nm	0.6-0.9	$7.1 \times 10^{11}$	$\sim 10^{-9}$	/	$1 \text{ mW}/\text{cm}^2$	9
	rGO/CQD/AgNP /Si	0.3 @940nm	0.36-0.94	$4.1 \times 10^{11}$	$\sim 10^{-9}$	556 ms/ 526 ms	$1 \mu\text{W}/\text{cm}^2 \sim$ $1 \text{ mW}/\text{cm}^2$	10
NN <sup>+</sup> /MS double junction structure and plasmonic enhanced	SiNWs/AgNPs	2.2 @980nm	0.254-2.2	$5.1 \times 10^{14}$	$\sim 2 \times 10^{-12}$	25/62	$1.4 \text{ nW}/\text{cm}^2 \sim$ $64.3 \text{ mW}/\text{cm}^2$	This work

$R$ ,  $D^*$ , and  $I_{dark}$  represent responsivity, specific detectivity, and dark current, respectively. rGO and CQD represent reduced graphene oxide, quantum dot.

## Supplementary References

- 1 A. Chandra, S. Giri, B. Das, S. Ghosh, S. Sarkar and K. K. Chattopadhyay, *Appl. Surf. Sci.*, 2021, **548**, 149256.
- 2 D. Wu, C. Jia, F. Shi, L. Zeng, P. Lin, L. Dong, Z. Shi, Y. Tian, X. Li and J. Jie, *J. Mater. Chem. A*, 2020, **8**, 3632-3642.
- 3 J. Mao, B. Zhang, Y. Shi, X. Wu, Y. He, D. Wu, J. Jie, C.-S. Lee and X. Zhang, *Adv. Funct. Mater.*, 2022, **32**, 2108174.
- 4 D. Wu, Y. Xu, H. Zhou, X. Feng, J. Zhang, X. Pan, Z. Gao, R. Wang, G. Ma, L. Tao, H. Wang, J. Duan, H. Wan, J. Zhang, L. Shen, H. Wang and T. Zhai, *InfoMat.*, 2022, **4**, e12320.
- 5 N. M. Devi, S. A. Lynrah, R. Rajkumari and N. K. Singh, *Sens. Actuators A: Phys.*, 2021, **327**, 112744.
- 6 K. Sarkar, P. Devi, A. Lata, V. K. Lokku and P. Kumar, *Adv. Opt. Mater.*, 2020, **8**, 2000228.
- 7 C.-H. Mao, A. Dubey, F.-J. Lee, C.-Y. Chen, S.-Y. Tang, A. Ranjan, M.-Y. Lu, Y.-L. Chueh, S. Gwo and T.-J. Yen, *ACS Appl. Mater. Interfaces*, 2021, **13**, 4126-4132.
- 8 B. Feng, J. Zhu, B. LU, F. Liu, L. Zhou and Y. Chen, *ACS Nano*, 2019, **13**, 8433-8441.
- 9 B. Du, W. Yang, Q. Jiang, H. Shan, D. Luo, B. Li, W. Tang, F. Lin, B. Shen, Q. Gong, X. Zhu, R. Zhu and Z. Fang, *Adv. Optical Mater.*, 2018, **6**, 1701271.
- 10 K. Sarkar, P. Devi, A. Lata, R. Ghosha and P. Kumar, *J. Mater. Chem. C*, 2019, **7**, 13182.